Flood Potential in the Southern Rocky Mountains Region and Beyond

Steven E. Yochum, Hydrologist, U.S. Forest Service, Fort Collins, Colorado
970-295-5285, steven.yochum@usda.gov

prepared for the SEDHYD-2019 conference, June 24-28th, Reno, Nevada, USA

Abstract

Understanding of the expected magnitudes and spatial variability of floods is essential for managing stream corridors. Utilizing the greater Southern Rocky Mountains region, a new method was developed to predict expected flood magnitudes and quantify spatial variability. In a variation of the envelope curve method, regressions of record peak discharges at long-term streamgages were used to predict the *expected flood potential* across zones of similar flood response and provide a framework for consistent comparison between zones through a flood potential index. Floods varied substantially, with the southern portion of Eastern Slopes and Great Plains zone experiencing floods, on average for a given watershed area, 15 times greater than an adjacent orographic-sheltered zone (mountain valleys of central Colorado and Northern New Mexico). The method facilitates the use of paleoflood data to extend predictions and provides a systematic approach for identifying extreme floods through comparison with large floods experienced by all streamgages within each zone. A variability index was developed to quantify within-zone flood variability and the flood potential index was combined with a flashiness index to yield a flood hazard index. Preliminary analyses performed in Texas, Missouri and Arkansas, northern Maine, northern California, and Puerto Rico indicate the method may have wide applicability. By leveraging data collected at streamgages in similar-responding nearby watersheds, these results can be used to predict expected large flood magnitudes at ungaged and insufficiently gaged locations, as well as for checking the results of statistical distributions at streamgaged locations, and for comparing flood risks across broad geographic extents.

Introduction

Greater insight into the expected magnitudes and spatial variability of floods is needed to more effectively manage our resources and build more sustainable communities. However, our understanding of floods is limited and hazards can be poorly communicated by technical specialists to decision makers and the public.

Generally, hydrologists and engineers rely on three methods for estimating flood magnitudes: 1) flood frequency methods that fit statistical distributions to annual peak discharge data and extrapolate these data to ungaged locations in regional regression studies; 2) rainfall-runoff based analyses; and 3) empirically-derived relationships between flood discharges and watershed characteristics (frequently implemented as envelope curves). Two of these methods rely directly on streamgage data. However streamgage databases can be problematic due to widely variable record lengths and periods, and mixed distributions of runoff mechanisms and flood magnitudes; this can be tricky for analyses and induces prediction uncertainty. As with other problems where predictions have substantial uncertainty, it's preferable to utilize multiple approaches. To this end, a new method was developed to help enhance understanding and communication of expected flood magnitudes and spatial variability.

Based on an analysis performed in the greater Southern Rocky Mountain region and preliminarily verified in several other regions of North America and Puerto Rico, a new method was developed using a space for time substitution to predict expected flood magnitudes at any given location given the streamgage record in similarly-responding nearby watersheds. Regressions of record peak discharges using drainage area and additional explanatory variables were fit across areas with similar flood records, with these areas referred to as *zones*. (The term zone is intentionally used to differentiate from regional regressions, which typically predict flood frequency relationships from streamgage analyses.) From these zonal regressions, a *flood potential index* was developed to rank flood hazards between zones, and a variability index was developed to quantify within-zone variability. Additionally, in combination with a flashiness index, an overall flood hazard index was developed. The method allows users to predict flood magnitudes and understand which areas tend to experience larger or smaller floods. This assists practitioners with answering such questions as:

- What magnitude of floods can be expected at a given ungaged location and how reasonable are predictions from the USGS regional regression equations?
- Is a streamgage flood frequency analysis providing reasonable results, or are the results biased due to such issues as the presence or absence of a large flood?
- Considering such applications as enhanced understanding of the geomorphic form and erosion hazard of stream corridors, the inherent risk of stream restoration, the impacts of wildfires, and the variability in probable maximum precipitation, what areas are prone to larger or smaller magnitude floods?
- Given the record of floods in the area, is a specific flood extreme in magnitude?
- Is a watershed that has only experienced relatively small floods in a precipitation shadow or has this watershed not yet experienced a larger flood that its neighboring watersheds indicate as being likely?

Methods

The primary study area consisted of the greater Southern Rocky Mountains, from the Great Plains of eastern Colorado to the Great Salt Lake, and from Casper, Wyoming to Albuquerque, New Mexico, with additional analyses on the Edwards Plateau (Texas Hill Country), the Ozark Plateau, northern Maine, Northern California, and northern Puerto Rico.

Streamgage data were obtained from the U.S. Geological Survey (USGS 2017a; USGS 2018a), a variety of state agencies, and the U.S. Bureau of Reclamation. Watershed areas up to 8600 km^2 (3320 mi^2) were evaluated. All streamgages with at least 40 years of record were required to be included in the analysis, with exceptions for redundant gages and gages dominated by attenuation from upstream reservoirs that have little or no pre-impoundment data. In areas with insufficient long-term streamgage data, streamgages with substantial floods but with records as short as 10 years were also used. Additional peak flow data were obtained for the 2013 Colorado Front Range flood (Jarrett, pers. comm. 2014, Schram 2014, Kimbrough and Holmes 2015, Moody 2016, Brogan et al. 2017, and Yochum et al. 2017).

Zones of relatively consistent flood magnitudes were developed, with the boundaries being approximate and often similar to the hydrologic region boundaries for regional regression equations (Miller, 2003; Kenney et al. 2007; Waltemeyer, 2008; Capesius and Stephens, 2009; Kohn et al., 2016). These boundaries were based on physiographic provinces and sections, watershed boundaries and topographic features, and flood flashiness.

Drainage area and other watershed characteristics were tested as regression predictors. Watersheds were delineated from modifications of HUC12 boundary datasets (USGS, 2017b). Arithmetic mean elevation, maximum elevation, and arithmetic mean slope and aspect

calculated in ArcGIS from 30 meter national elevation datasets (USGS 2017b). Annual and monthly area-weighted precipitation was computed from 30-year, 800 meter PRISM grids (Daly et al. 2008; PRISM 2018).

Four indices were used for comparing floods between zones. The flood potential index (P_f) is:

$$P_f = Average\left({Q_{20}}/{4.15} + {Q_{200}}/{21.0} + {Q_{2000}}/{106}\right)$$

, where Q_{20} is the fitted discharge (m^3/s) for a 20 km^2 watershed for the zone of interest (which is divided by the fitted discharge for a 20 km^2 watershed in zone 2), and with 200 and 2000 noting similar computations for 200 and 2000 km^2 watersheds. The variability index (V_f) is the ratio of the regression intercepts for maximum likely flood potential and the expected flood potential, specifically:

$$V_f = {a_{mlf}}/{a_{efp}}$$

, where $Q = aA^b$. Flashiness was determined using the Beard flash flood index (F; Beard 1975), which is computed as the standard deviation of the natural logarithms of the annual peak flow for each streamgage. A flood hazard index (H_f) was computed as:

$$H_f = P_f * F$$

Regressions were performed using the R software package. Natural logarithmic transformations were applied, which generally provided good adherence to regression assumptions of linearity, homoscedasticity, and independent and normally-distributed residuals. Where encountered, outliers were assumed to not be errors and were identified using Cook's distance (D) measurement of influence. High outliers were typically retained to maintain conservative predictions. In zones where low outliers were excluded, these points were identified where D > 1.9*(mean D). Low outliers exclusion was necessary to avoid developing models with less conservative flood predictions.

Additional details on the methods utilized in the analysis are provided in Yochum et al. (in review).

Results and Discussion

Enhanced understanding of the magnitude and spatial variability of flood hazards and simpler language for communicating these hazards with managers and the public are needed to help protect lives, property, and infrastructure. Data exploration of streamgage annual peak discharge data revealed a spatial pattern in experienced floods. Regressions of the maximum (record) peak discharges (Q) using watershed area (A), topographic, and climatologic predictors were performed across zones of similar flood response, with high levels of explained variance (Table 1). The method facilitates understanding of floods that, given these precedents, are likely to occur in the future across each zonal extent. Detailed analyses have been completed for the greater Southern Rocky Mountains region and preliminary analyses were performed in diverse regions across the United States.

In the greater Southern Rocky Mountains region (Figure 1), regressions were performed for eleven zones of similar flood responses. The analyses included 463 streamgages with watershed areas ranging from 1.5 to 8550 km^2 (0.58 to 3300 mi^2). Each of these regressions define the *expected flood potential* for each zone using a method independent of flood frequency analyses; Figure 2 provides example plots for four zones, with additional information available in Yochum et al. (in review). Up to 93% of the variance in the record peak discharges was explained using up to two predictors, with the prediction equations provided on each plot. Using a space for time substitution, this method predicts flood magnitudes that can be expected in specific watersheds

(within the derived watershed area range) given the streamgage record of appropriate neighboring watersheds, providing a complimentary approach to flood frequency/regional regression and rainfall-runoff models, and potentially reducing uncertainties in predicting the size of large floods.

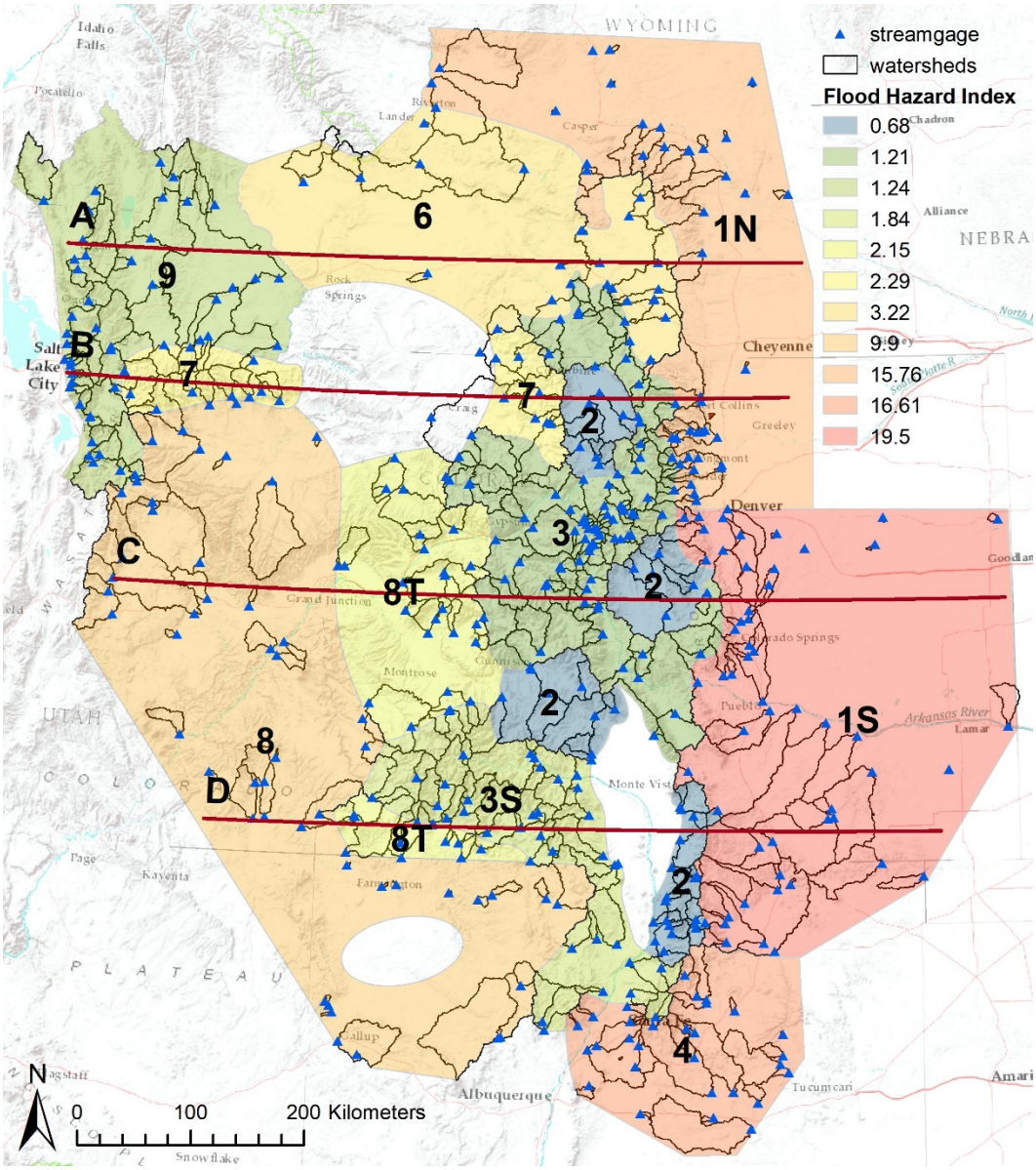

Figure 1. Greater Southern Rocky Mountains analysis extent, with zone boundaries, utilized streamgages, and watershed boundaries. The colors represent the flood hazard index value for each zone. Embedded areas with insufficient data do not have any coloring. Section lines are also indicated.

Table 1: Expected flood potential analysis results, where n is the number of streamgages in each regression, R^2 is the explained variance, P_f is the flood potential index, F is the Beard flash flood index, and H_f is the flood hazard index.

	Zone	ID	n	R^2	P_f	V_f	F	H_f
Southern Rocky Mountains Region	Eastern Slopes & Great Plains, South	1S	45	0.70	15.0	2.77	1.30	20
	Eastern Slopes & Great Plains, North	1N	41	0.75	13.8	1.76	1.14	16
	Orographic Sheltered	2	36	0.89	1.0	1.52	0.69	0.7
	Southern Rocky Mountains	3	90	0.93	2.3	1.62	0.53	1.2
	Southern Rocky Mountains, South	3S	45	0.71	3.0	1.94	0.61	1.8
	Southern Transition	4	25	0.85	14.0	1.97	1.19	17
	Wyoming Basin	6	21	0.90	3.6	1.43	0.90	3.2
	Northwest Mountains	7	21	0.85	4.7	1.38	0.49	2.3
	Colorado Plateaus	8	42	0.74	9.0	1.88	1.10	10
	Colorado Plateaus Transition	8T	27	0.81	2.7	1.50	0.80	2.2
	Wasach and West Basins	9	41	0.79	1.9	1.78	0.65	1.2
Preliminary Analyses	Great Basin Transition	22	29	0.87	2.9	----	1.10	3.2
	Sierra Nevada Mountains	23	56	0.91	12.7	----	1.07	14
	California Coastal Ranges	25	30	0.98	33.3	----	0.71	24
	Eastern Klamath Mountains	26	15	0.98	17.2	----	0.84	14
	Midwest, Central Lowlands	51	16	0.95	22.7	----	0.72	16
	Ozark Plateaus	52	19	0.92	34.0	----	0.82	28
	Edwards Plateau	61	16	0.98	79.4	----	1.90	151
	New England, Coastal Lowlands and Uplands	95	19	0.96	5.5	----	0.39	2.1
	Puerto Rico	101	21	0.97	117	----	0.88	103

Upper 95% prediction limits were utilized to understand flood variability within each zone, with this limit dubbed the *maximum likely flood potential*. Floods above this level are unlikely but still possible, and are considered extreme – this method provides a tool for quantitatively and consistently defining extreme floods. The amount of departure above the maximum likely flood potential denotes the degree of extremity. For example, in the Eastern Slopes and Great Plains South (zone 1S; Figure 1; Figure 2-A), an area that has experienced the largest and most variable flood magnitudes within the greater Southern Rocky Mountains analysis extent, four extreme floods occurred at the evaluated streamgages. The most extreme flood was experienced on Jimmy Camp Creek, CO in June of 1965 (Q = 3510 m^3/s = 124,000 ft^3/s; A = 169 km^2 = 65 mi^2), with the second most extreme flood occurring on Kiowa Creek in May of 1935 (Q = 1230 m^3/s = 43,500 ft^3/s, A = 74 km^2 = 29 mi^2). Generally, extreme floods tend to be associated with intense thunderstorms, squall lines, and shortwave troughs developed within or influenced by synoptic-scale weather systems, and are often associated with atmospheric blocking patterns (Hirschboeck, 1987).

There is substantial variability in the expected flood potential across this regional analysis extent (Figure 3); Table 2 provides expected flood potential and maximum likely flood potential predictions for a standard 1000 km^2 watershed size. This variability is despite these zones relatively close (or adjacent) proximity to each other (Figure 1, Figure 4) and may be due to watershed characteristics, such as bedrock exposure, thin soils, vegetative conditions, and steep relief (Osterkamp & Friedman 2000; O'Connor & Costa 2004), as well as flood type (rainfall versus snowmelt), orographic blockage (rain shadow), water vapor sources, rainfall rates, and convective storm sizes.

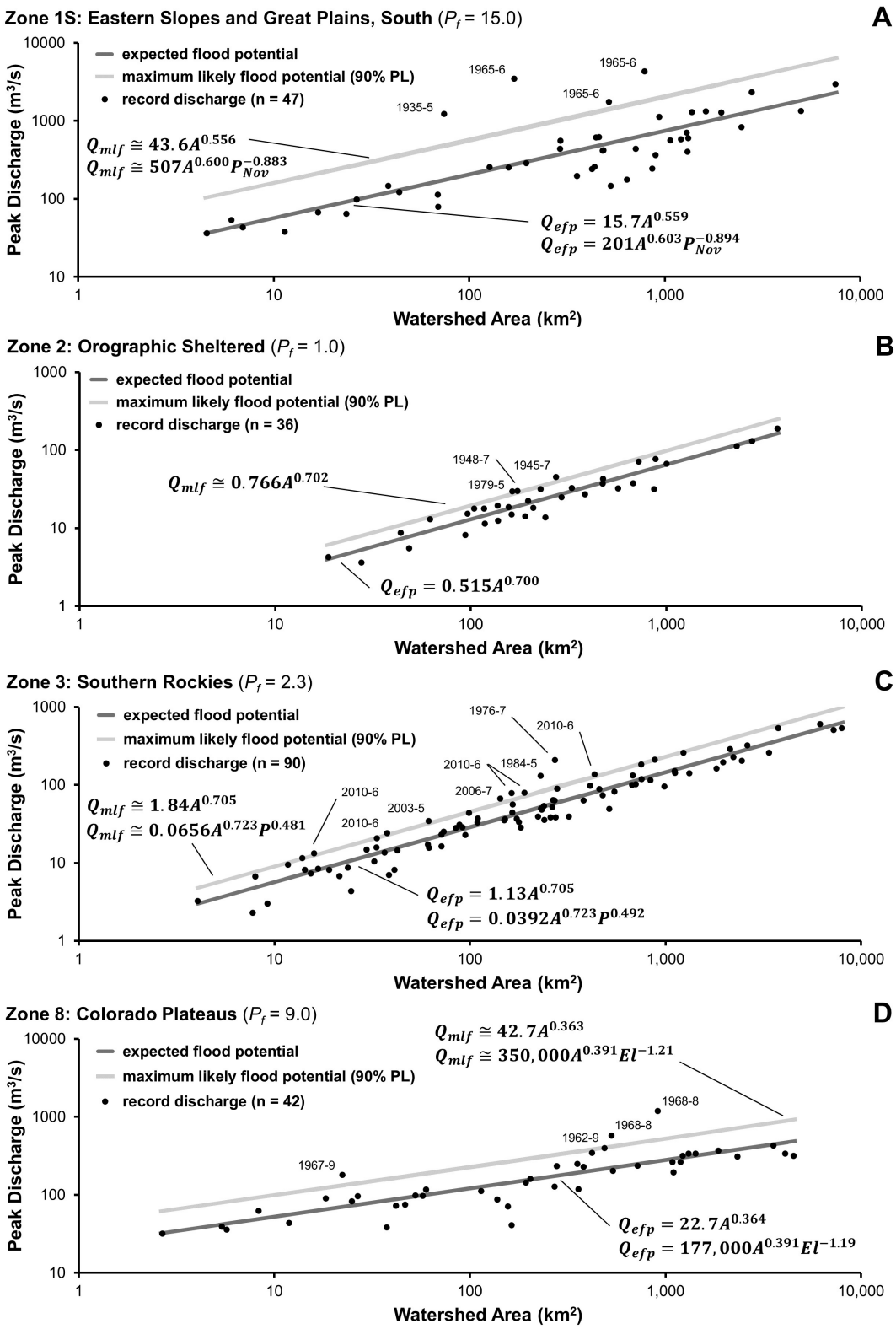

Figure 2. Selected zone plots of long term streamgage record peak discharges (black dots), expected flood potential (regression fit), and the maximum likely flood potential (90% prediction limit). Dates of extreme floods are also provided. A: watershed area (km²); P: average annual precipitation (mm); P_{Nov}: average November precipitation (mm); El: average watershed elevation (m).

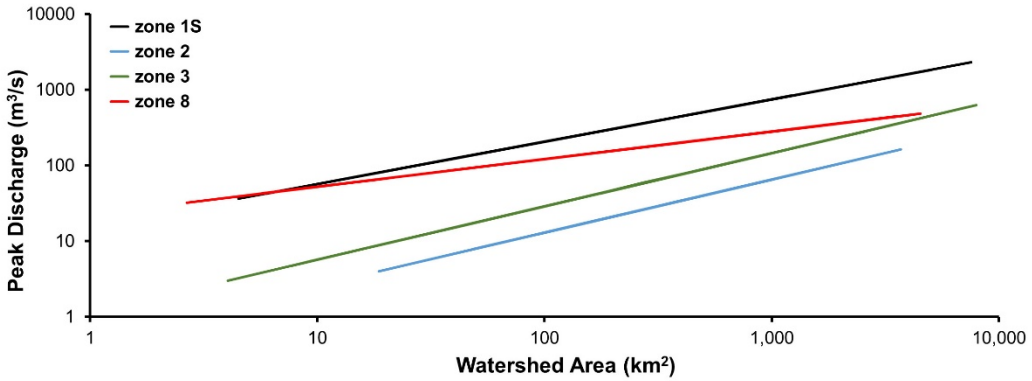

Figure 3. Expected flood potential for zones 1s (Eastern Slopes and Great Plains, South), 2 (Orographic Sheltered), 3 (Southern Rockies), and 8 (Colorado Plateaus).

Table 2. Expected flood potential and maximum likely flood potential flood magnitude estimates for a standard 1000 km² (386 mi²) watershed.

		Expected Flood Potential		Maximim Likely Flood Potential	
Zone	**ID**	(m^3/s)	(ft^3/s)	(m^3/s)	(ft^3/s)
Eastern Slopes & Great Plains, South	1S	750	26,000	2,000	71,000
Orographic Sheltered	2	65	2,300	98	3,500
Southern Rocky Mountains	3	150	5,100	240	8,500
Colorado Plateaus	8	280	9,900	520	18,000

Indices were used to quantify the spatial variability of flood hazards across diverse topographic areas. The *flood potential index* (P_f) compares the expected flood potential to the zone with the smallest experienced floods (zone 2, Orographic Sheltered). Zone 2 is composed of the high-elevation rain-shadowed valleys of central Colorado and northern New Mexico, specifically North Park, South Park, and the upper Gunnison, San Luis, and Taos valleys (Figure 1). This index varied from 1.0 to 15 for the core study area (Table 1), with the highest flood potential zone (1S) experiencing floods, on average, 15 times greater than the adjacent Orographic Sheltered zone. The *flood variability index* (V_f) quantifies the variability of the within-zone record discharges (Figure 2); the greatest variability was in zone 1S and the least in zone 7 (Northwest Mountains). The *Beard flashiness index* (F) was utilized to quantify how unexpectedly large a flood can be compared to more typical floods. The zonal average F varied from 0.49 to 1.30 (in zone 1S), with higher values indicating greater flashiness. The *flood hazard index* (H_f) is the product of P_f and F, and accounts for both the flood magnitude and flashiness. H_f varied from 0.7 to 20, with the least flood hazards in zone 2 and the greatest in zone 1S. Other areas of the greater Southern Rocky Mountains region with highest flood potential and hazard are zones 1N and 4, with zone 8 also being of note (Figure 1). These zones include numerous urban areas, including cities along the Colorado Front Range (Denver, Colorado Springs, Fort Collins, Boulder), Casper and Cheyenne, WY, as well as Pueblo and Trinidad, CO, Santa Fe and Farmington, NM, and Moab, UT.

Four cross sections were cut from west to east across the study area (Figure 1), to illustrate how flood potential varies with topographic landforms (Figure 4). The eastern and southwestern portions of the study area have the highest flood potential, while the highest elevations (and the embedded valleys) have the lowest flood potential. These differences may likely be the result of dominant meteorological processes induced by the mountainous terrain of the study area.

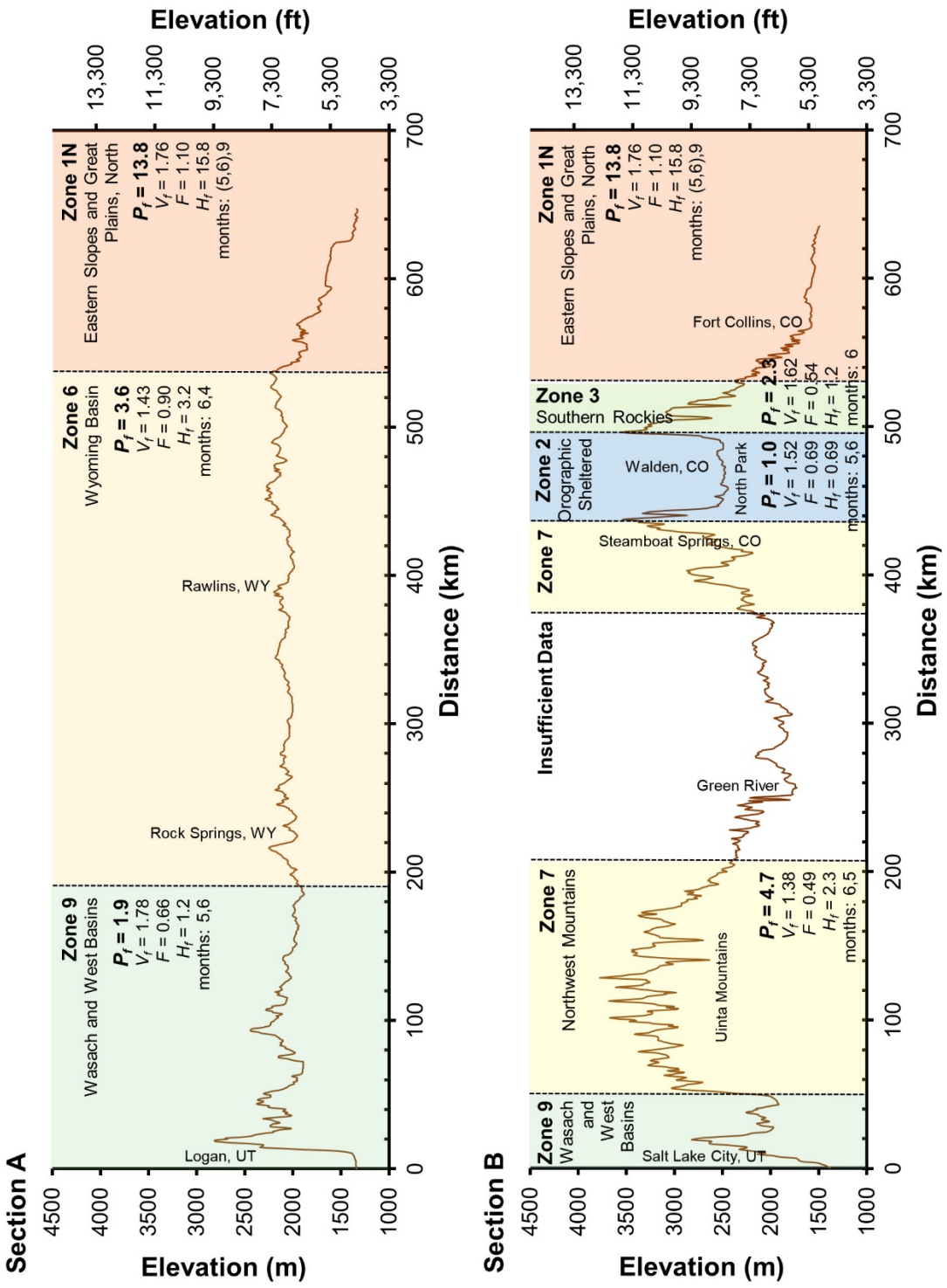

Figure 4a. Cross sections across the study area, from west to east, showing relief as well as flood potential and other indices. Warmer and cooler colors indicate higher and lower flood potential, respectively.

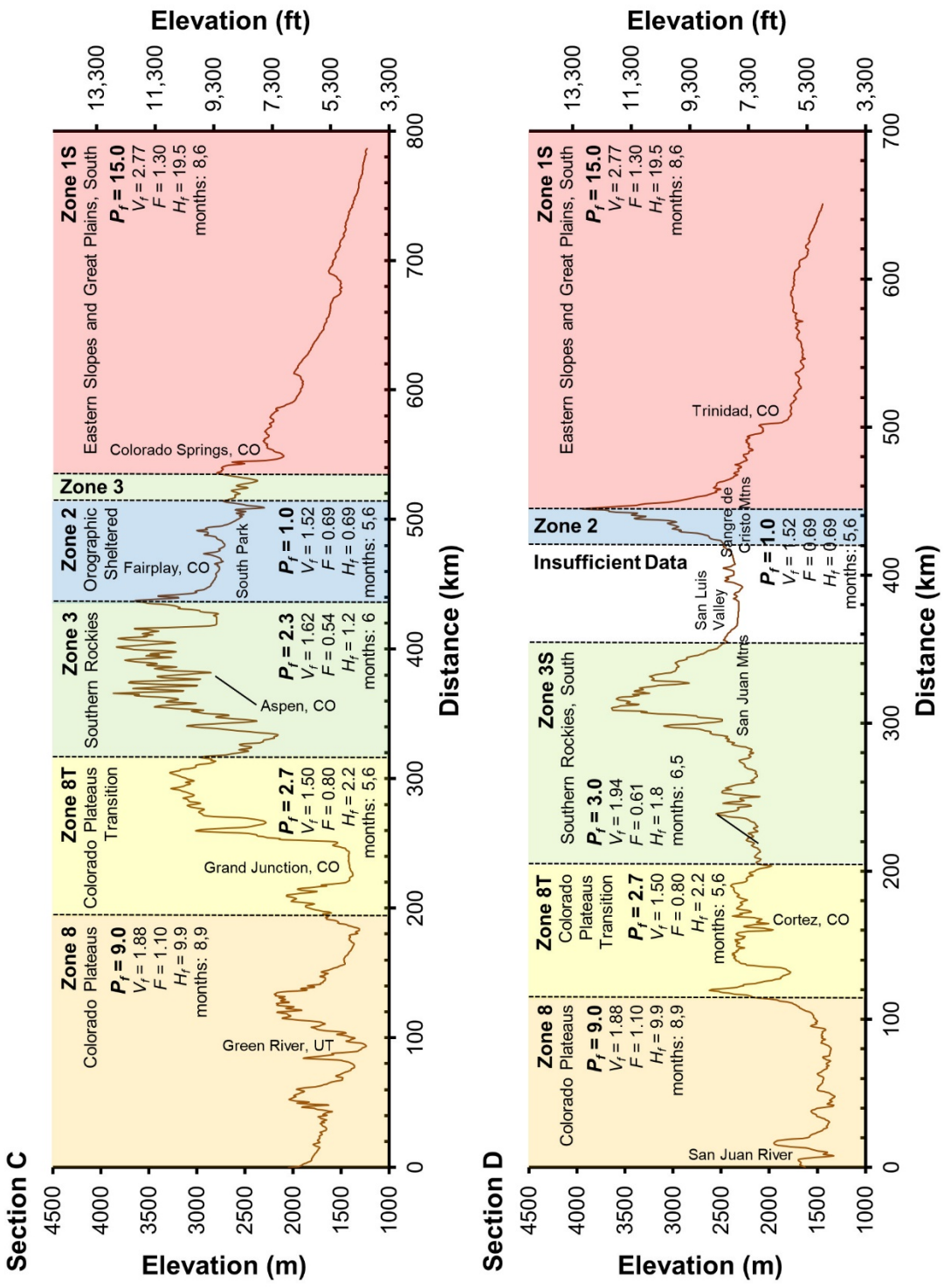

Figure 4b. Cross sections across the study area, from west to east, showing relief as well as flood potential and other indices. Warmer and cooler colors indicate higher and lower flood potential, respectively.

Northern Colorado Front Range Floods

The northern Colorado Front Range is part of zone 1N (Eastern Slopes and Great Plains, North). This area is of special interest due to the well-known Big Thompson Flood of 1976 and 2013 Colorado Front Range floods (Gochis et al. 2015; Yochum et al. 2017). Initially, the 2013 floods were referred to by the National Weather Service as an event with "biblical rainfall amounts" (Koronowski 2013), with rainfall on the order of a 1000-year storm (NWS 2013). Such overly sensational language is problematic in that, upon hearing this, citizens frequently react by considering the flooding to be an aberration, discounting the possibility of future occurrences and inhibiting the development of more resilient stream valley communities. Flood potential analyses allow us to place a flood event into a broader perspective that considers other floods that have been measured in neighboring (zonal) watersheds.

The expected flood potential regression is illustrated in Figure 5, which includes the record peak discharges (black dots), the maximum likely flood potential (dark gray line), and a number of the most substantial peak flow estimates collected after the 2013 (and 1997) floods (marked with a "+"). The most extreme floods (Figure 6), in decreasing order of extremity, were on Sand Creek, WY (August 1955), the Spring Creek Flood in Fort Collins, CO (July 1997), and the Big Thompson flood (July 1976). The other extreme floods were experienced in September of 2013 in the St. Vrain Creek and in Little Thompson River watersheds. Other areas impacted by the 2013 flood experienced magnitudes that were similar to (or less than) the expected flood potential. Hence, most portions of the 2013 flood extent did not experience extreme floods, but rather flood magnitudes that can be considered expected given the available zonal streamgage records.

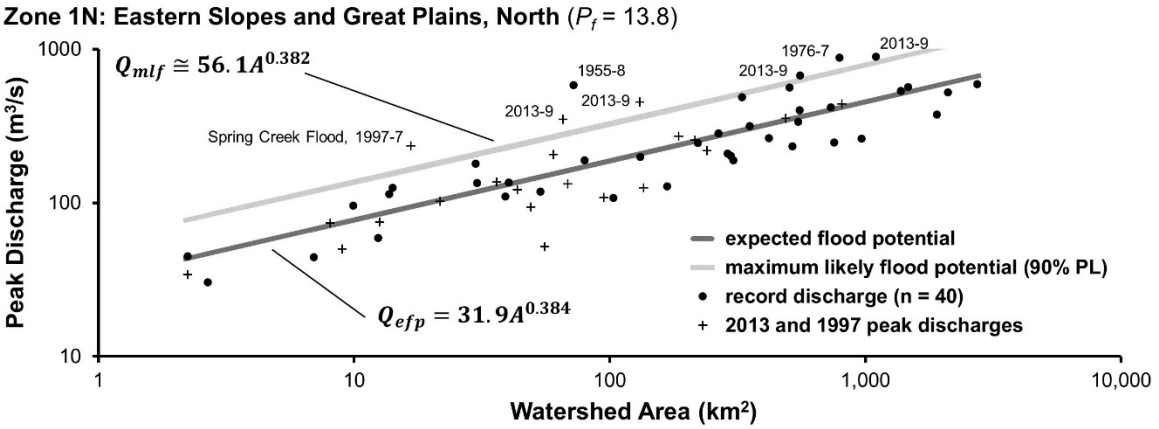

Figure 5. Zone 1N plot of long term streamgage record peak discharges (black dots), expected flood potential (regression fit), and the maximum likely flood potential (90% prediction limit). Floods greater than the maximum likely flood potential are considered extreme, with the departure indicating the degree of extremity. Flood peaks at non-streamgaged locations are marked with a "+". Dates of extreme floods are also provided.

An interesting characteristic of the Colorado Front Range is that, at higher elevations as the continental divide is approached, flood potential decreases. Traditionally, a rule of thumb that a 2300 m (7500 ft) elevation contour is the approximate boundary between snowmelt (zone 3) and rainfall-dominated floods (Follansbee & Sawyer 1948, Jarrett 1990), with the rainfall floods having much greater flood potential. It has been hypothesized that as a warm, moist airmass is forced upslope by the mountains, this topography initially intensifies precipitation rates due to orographic lifting (as illustrated by the eastern portions of the sections in Figure 4), but as the airmass rises still higher further west, available moisture in the air column tends to decrease and precipitation rates decrease (Hansen et al., 1988, Osterkamp & Friedman, 2000). However,

large magnitude 2013 flooding in higher-elevation areas of the Big Thompson watershed indicated the limitations of this rule of thumb. Additional exceptions to the 2300 m hypothesis were noted by Smith et al. (2018). Reflecting this, the zonal boundary between zone 1N and 3 (Figure 6) is not a contour but is, instead, a series of topographic features that appear to block moisture availability and reduce convection and precipitation intensity.

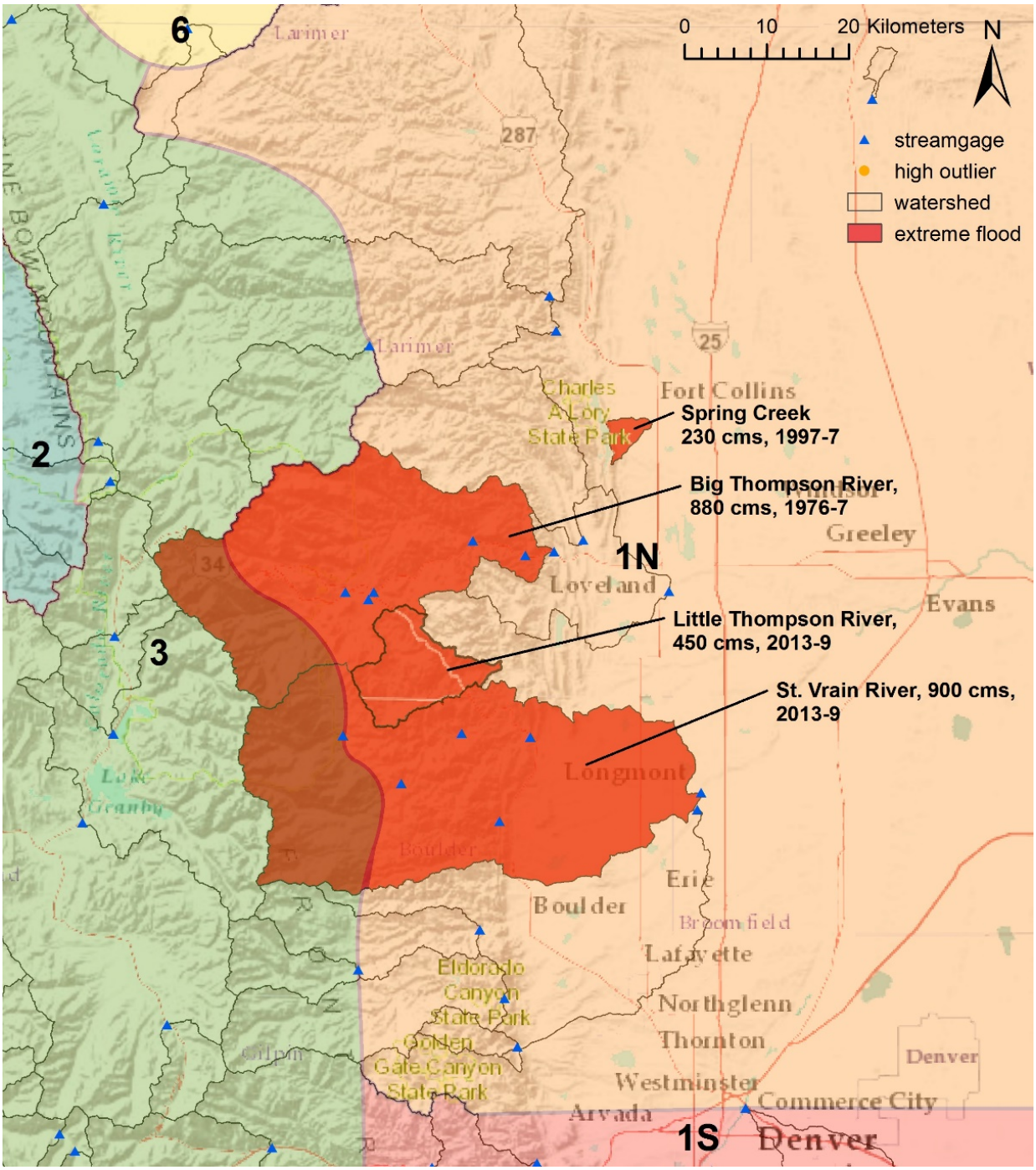

Figure 6. Portion of zone 1N (Eastern Slopes and Great Plains, North) impacted by the floods of 1976 (Big Thompson), 1997 (Spring Creek), and 2013 (Colorado Front Range flood). Watersheds that experienced extreme floods are highlighted in red. The most extreme flood in this zone was experienced outside this map extent, on Sand Creek, Wyoming.

Broader Application

Preliminary analyses were performed across diverse areas of the United States, to assess broader applicability of the technique. These areas included the southern Midwest, northern New England, central Texas, northern California, and Puerto Rico (Figure 7). Distinct zonal variability in flood potential was identified with high-levels of explained variance (Table 1). Preliminary flood potential indices varied from the low values of 2.9 (Great Basin Transition, leeward side of the Sierra Nevada and southern Cascade Mountains) and 5.5 (northern New England), with increased flood potential in the Sierra Nevada Mountains (P_f = 13), the California Coastal Ranges (P_f = 33), and the southern Midwest (P_f = 34 in the Ozarks). Still higher flood potential was quantified on the Edwards Plateau of Texas (P_f = 79) and Puerto Rico (P_f = 117), which has experienced the largest floods within the current investigation. Additionally, this method allows the simple comparison of flood potential between any two zones. For example, the Edwards Plateau (which includes the Texas hill country) experiences, on average for a given watershed area, 79 times larger floods than the index zone and 79/15 = 5.3 times larger floods than the zone with the largest flood magnitudes in the greater Southern Rocky Mountains region, the Eastern Slopes and Great Plains, South (zone 1S). This method shows promise for comparing flood variability on a continental scale.

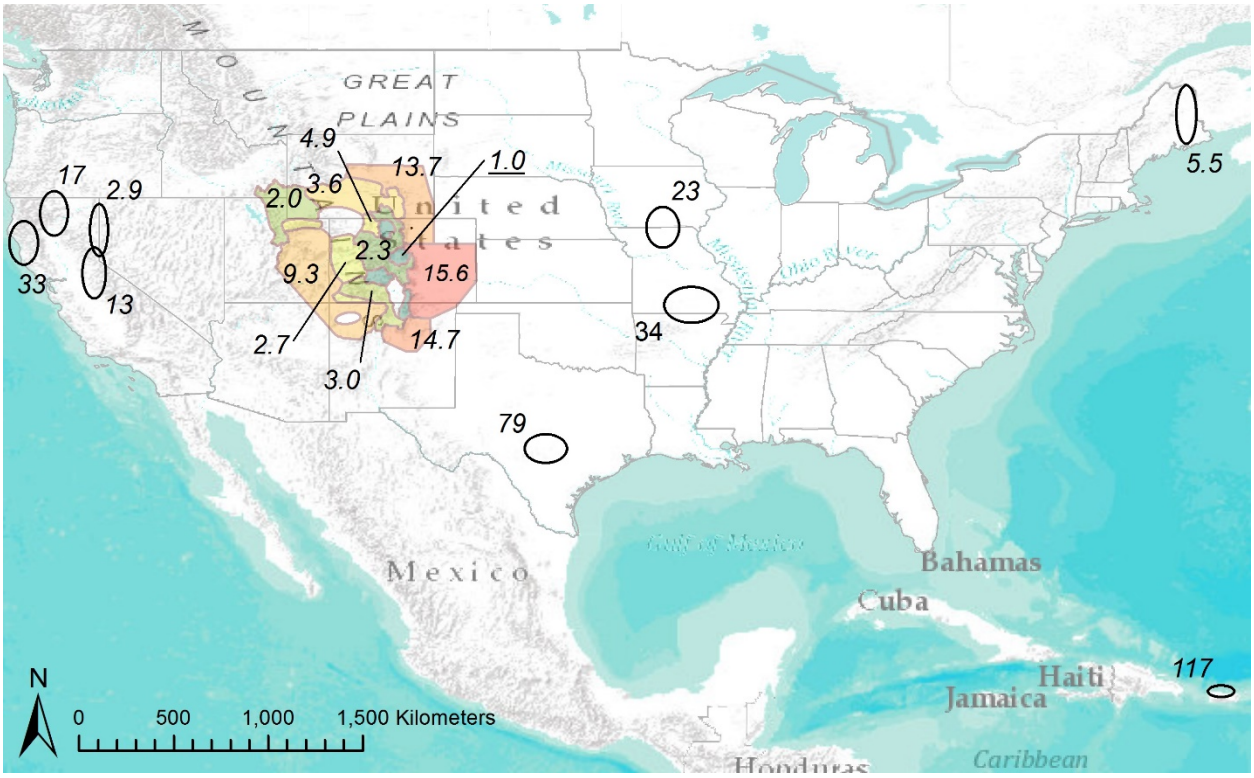

Figure 7. Flood potential index values for the greater Southern Rocky Mountains region analysis extent and the broader application areas (preliminary). The ovals represent the general area of analyses, not specific zone extents. The underlined 1.0 value indicates the index zone (large Central Colorado and northern New Mexico mountain valleys).

Flashiness also varied between the different analyzed zones. The lowest flashiness is experienced in northern New England (F = 0.39) and the highest on the Edwards Plateau (F = 1.90). The variability in both flood potential and flashiness is illustrated in Figure 8, which shows preliminary results for all currently analyzed areas. Zones in the upper-right portion of this figure have the greatest flood hazard (61 – Edwards Plateau, 101 – Puerto Rico), while zones in

the lower-left portion of the figure have the least flood hazard (3 – Southern Rocky Mountains, 7 – Northwest Mountains of the greater Southern Rocky Mountain region, 95 – northern New England). The flood hazard index subsumes this into a single numerical value, with the Edwards Plateau indicating the greatest flood hazard (H_f = 151) and the index area zone 2 (Orographic Sheltered) having the least hazard (H_f = 0.7) across the current analysis extent.

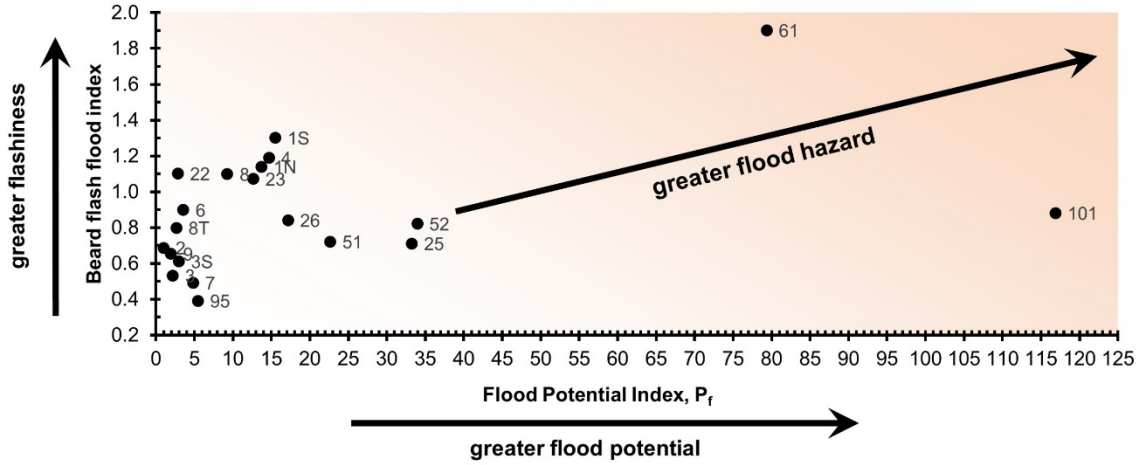

Figure 8. Flood hazard comparison of analyzed zones (identified by the provided ID numbers), with hazard composed of the flood potential and the Beard flash flood indices. The greatest flood hazard index for these preliminary extended analyses is the Edward Plateau (zone 61), Texas (H_f = 151).

Conclusions

Using streamgage records at long term stations, regressions of record peak discharges across zones of similar flood response were utilized to define the *expected flood potential*, a term developed to help understand and communicate what flood discharge magnitudes can be expected given the streamgage records of nearby watersheds. These zones were delineated using physiographic provinces, watershed boundaries and topographic features, and flood flashiness. The method was developed for the greater Southern Rocky Mountain region, with additional preliminary analyses performed across diverse areas of the United States. Upper 90% prediction limits were used to define the *maximum likely flood potential* and to assess flood variability. The 90% prediction limits also identify extreme floods, with departure above this level denoting the degree of extremity. Indices were used to quantify the variability of flood hazards, with the areas with the greatest hazards (in increasing magnitude) being the Southern Rocky Mountains eastern slopes and adjacent Great Plains, the California Coastal Ranges, the Ozark Plateau, Puerto Rico, and the Edwards Plateau of Texas. This methodology shows promise for providing practitioners, managers, and the public with valuable additional information for developing more resilient stream valley communities. Additionally, this method provides indices and language that can enhance communication among scientists, for developing greater understanding of the mechanisms that cause large floods and how these mechanisms may change over time due to global warming.

Acknowledgements

Julian Scott and David Levinson contributed to this work; their efforts are highly valued. Additionally, both David Levinson and Ann Banitt are appreciated for their reviews of this report.

References

Beard, L.R. 1975. Generalized evaluation of flood potential. University of Texas, Austin, Center for Research in Water Resources. CRWW-124, pp 1-27.

Brogan, D.J., Nelson, P.A., MacDonald, L.H. 2017. Reconstructing extreme post-wildfire floods: a comparison of convective and mesoscale events. Earth Surface Processes and Landforms 42, 2505-2522, doi:10.1002/esp.4194.

Capesius, J.P., Stephens, V.C. 2009. Regional regression equations for estimation of natural streamflow statistics in Colorado. U.S. Geological Survey Scientific Investigations Report 2009–5136.

Daly, C., Halbleib, M., Smith, J.I., Gibson, W.P., Doggett, M.K., Taylor, G.H., Curtis, J., and Pasteris, P.A. 2008. Physiographically-sensitive mapping of temperature and precipitation across the conterminous United States, International Journal of Climatology, 28: 2031-2064.

Follansbee, R., & Sawyer, L.R. 1948. Floods in Colorado. U.S. Department of Interior, Geological Survey. Water Supply Paper 997.

Gochis, D., Schumacher, R., Friedrich, K., Doesken, N., Kelsch, M., Sun, J., Ikeda, K., Lindsey, D., Wood, D., Dolan, B., Matrosov, S., Newman, A., Mahoney, K., Rutledge, S., Johnson, R., Kucera, P., Kennedy, P., Sempere-Torres, D., Steiner, M., Roberts, R., Wilson, J., Yu, W., Chandrasekar, V., Rasmussen, R., Anderson, A., & Brown, B. 2015. The Great Colorado Flood of September 2013. Bulletin of the American Meteorological Society, 96, 1461–1487.

Hansen, E.M., Fenn, D.D., Schreiner, L.C., Stodt, R.W., & Miller, J.F. 1988. Probable maximum precipitation estimates – United States between the continental divide and the 103rd meridian. National Oceanic and Atmospheric Administration, Hydrometeorological Report No. 55A.

Hirschboeck, K.K. 1987. Catastrophic flooding and atmospheric circulation anomalies, in Mayer, L. and Nash, D.B., eds., Catastrophic Flooding, Allen & Unwin, pp 23-56.

Jarrett, R.D. 1990. Paleohydrolgic techniques used to define spatial occurrence of floods. Geomorphology 3, 181-195.

Jarrett, R.D. 2014. personal communication, Applied Weather Associates.

Kenney, T.A., Wilkowske, C.D., Wright, S.J. 2007. Methods for estimating magnitude and frequency of peak flows for natural streams in Utah. U.S Geological Survey Scientific Investigations Report 2007–5158.

Kimbrough, R.A., Holmes, R.R. 2015. Flooding in the South Platte River and Fountain Creek Basins in Eastern Colorado, September 9-18, 2013. U.S. Department of Interior, U.S. Geological Survey, Scientific Investigations Report 2015-5119.

Kohn, M.S., Stevens, M.R., Harden, T.M., Godaire, J.E., Klinger, R.E., Mommandi, A. 2016. Paleoflood investigations to improve peak-streamflow regional-regression equations for natural streamflow in Eastern Colorado, 2015. U.S. Geological Survey Scientific Investigations Report 2016-5099.

Koronowski, R. 2013 'Biblical' Amounts Of Rainfall Slam Colorado, Causing Death, Destruction, And Massive Flooding. https://thinkprogress.org/biblical-amounts-of-rainfall-slam-colorado-causing-death-destruction-and-massive-flooding-422e62aaa260/.

Miller, K.A. 2003. Peak-flow characteristics of Wyoming streams. U.S Geological Survey Water-Resources Investigations Report 03-4107.

Moody, J.A. 2016. Estimates of Peak Discharge for 21 Sites in the Front Range in Colorado in Response to Extreme Rainfall in September 2013. U.S. Geological Survey Scientific Investigations Report 2016-5003, doi:10.3133/sir20165003.

National Weather Service (NWS) 2013. Exceedance Probability Analysis for the Colorado Flood Event, 9 - 16 September 2013. National Oceanic and Atmospheric Administration, National Weather Service, Hydrometeorological Design Studies Center.

O'Connor, J.E., Costa, J.E. 2004. Spatial distribution of the largest rainfall-runoff floods from basins between 2.6 and 26,000 km2 in the United States and Puerto Rico. Water Resources Research 40, W01107, doi:10.1029/2003WR002247.
Osterkamp, W.R., Friedman, J.M. 2000. The disparity between extreme rainfall events and rare floods – with emphasis on the semi-arid American West. Hydrological Processes 14, 2817-2829.
PRISM Climate Group, Northwest Alliance for Computational Science and Engineering, 30-Year Normals. http://www.prism.oregonstate.edu/normals/ (accessed August 2018).
Schram, H., Wulliman, J.T., Rapp, D.N. 2014. Hydrologic Evaluation of the St. Vrain Watershed: Post September 2013 Flood Event. Prepared for the Colorado Department of Transportation, Region 4 Flood Recovery Office. Jacobs Engineering, Denver, Colorado.
Smith, J.A., Cox, A.A., Baeck, M.L, Yang, L., & Bates, P. 2018. Strange floods: The upper tail of flood peaks in the United States. Water Resources Research. doi:10.1029/2018WR022539.
U.S. Geological Survey (a). Peak Streamflow for the Nation. Retrieved from https://nwis.waterdata.usgs.gov/usa/nwis/peak (accessed August 2017).
U.S. Geological Survey (b). Peak Streamflow for the Nation. Retrieved from https://nwis.waterdata.usgs.gov/usa/nwis/peak (accessed October 2018).
U.S. Geological Survey (b). Watershed Boundary Dataset. Retrieved from https://nhd.usgs.gov/wbd.html (accessed December 2017).
Waltemeyer, S.D. 2008. Analysis of the magnitude and frequency of peak discharge and maximum observed peak discharge in New Mexico and surrounding areas. U.S Geological Survey Scientific Investigations Report 2008-5119.
Yochum, S.E., Sholtes, J.S., Scott, J.A., Bledsoe, B.P. 2017. Stream power framework for predicting geomorphic change: The 2013 Colorado Front Range flood. Geomorphology 292, 178-192.
Yochum, S.E., Scott, J.A., Levinson, D.H. In review. Methods for Assessing Expected Flood Potential and Variability: Southern Rocky Mountains Region. Water Resources Research.